

Probabilistic Approaches to Alignment with Tandem Repeats

Michal Nánási, Tomáš Vinař, and Broňa Brejová

Faculty of Mathematics, Physics, and Informatics, Comenius University,
Mlynská dolina, 842 48 Bratislava, Slovakia

Abstract. We propose a simple tractable pair hidden Markov model for pairwise sequence alignment that accounts for the presence of short tandem repeats. Using the framework of gain functions, we design several optimization criteria for decoding this model and describe the resulting decoding algorithms, ranging from the traditional Viterbi and posterior decoding to block-based decoding algorithms specialized for our model. We compare the accuracy of individual decoding algorithms on simulated data and find our approach superior to the classical three-state pair HMM in simulations.

1 Introduction

In this paper, we explore the use of pair hidden Markov models (pair HMMs, PHMMs) in improving the quality of pairwise sequence alignment in the presence of tandem repeats. We propose a simple tractable model that explicitly accounts for short tandem repeats, and we use the framework of maximum expected gain to explore a variety of decoding optimization criteria for our model.

Pair HMMs have for a long time played a major role in sequence alignment (Durbin et al., 1998). The traditional Needleman-Wunsch algorithm (Needleman and Wunsch, 1970) and its variants can be easily formulated as a special case of alignment with PHMMs (we call this approach Viterbi decoding). The main advantage of PHMMs is that they allow to express the scoring scheme in a principled way in the context of a probabilistic model.

Sequence alignments are a mainstay of comparative genomics. By comparing sequences that evolved from a common ancestor, we can infer their phylogenetic relationships, discover sites under functional constraint, or even shed light on the function of individual sequence elements. However, comparative genomic methods are very sensitive to the quality of underlying alignments, and even slight inaccuracies may lead to artifacts in the results of comparative methods.

It is very difficult to evaluate alignment accuracy, yet even simple statistics can reveal artifacts of present-day algorithms. Lunter et al. (2008) demonstrated systematic biases caused by the optimization criteria set by the Needleman-Wunsch approach. They show that by using variants of the posterior decoding instead of the traditional Viterbi algorithm, one can significantly increase the quality of alignments. While the Viterbi decoding seeks one highest scoring

alignment, the posterior decoding summarizes information from all alignments of the two sequences. This approach was also found superior by other authors (Miyazawa, 1995; Holmes and Durbin, 1998; Schwartz and Pachter, 2007).

An algorithm by Hudek (2010) is an intermediate between the Viterbi and posterior decoding, summarizing probabilities of alignments within short blocks. The goal is to segment the alignment into blocks, where each block has gaps in only one of the two sequences. The decoding algorithm considers each block as a unit, summing probabilities of all alignments that had the same block structure. Finally, Satija et al. (2010) have demonstrated that fixing a particular alignment is not necessary in some comparative genomics applications, instead one can consider all possible alignments weighted by their probability in the PHMM.

In this paper, we concentrate on modeling sequence alignments in the presence of tandem repeats. Short tandem repeats cover more than 2% of the human genome, and occur in many genes and regulatory regions (Gemayel et al., 2010); in fact, majority of recent short insertions in human are due to tandem duplication (Messer and Arndt, 2007). Evolution of tandem repeats is dominated by tandem segmental duplications resulting in regions composed of a highly variable number of almost exact copies of a short segment. Such sequences are difficult to align with standard scoring schemes, because it is not clear which copies from the two organisms are orthologous. Misalignments due to the presence of short tandem repeats are usually not limited to the repetitive sequence itself, but may spread into neighbouring areas and impact the overall alignment quality.

Sequence alignment with tandem duplication was first studied by Benson (1997). They propose an extension of the traditional Needleman-Wunsch algorithm that can accommodate tandem repeats in $O(n^4)$ time. They also propose several faster heuristic algorithms. Additional work in this area concentrated on computing variants of edit distance either on whole sequences with tandem arrays or on two tandem arrays using different sets of evolutionary operations (Sammeth and Stoye, 2006; Bérard et al., 2006; Freschi and Bogliolo, 2012).

The first probabilistic approach to alignment of tandem duplications was introduced by Hickey and Blanchette (2011), who developed a new probabilistic model by combining PHMMs with Tree Adjoining Grammars (TAGs). Their model favors tandem duplications to other insertions, but the approach does not explicitly model whole arrays of tandemly repeated motifs. Moreover, algorithms to train and decode such models are relatively complex.

Protein sequences with repetitive motifs (such as zinc finger proteins) are a special class of proteins and their alignment has many features in common with DNA sequence alignment with tandem repeats. Kováč et al. (2012) combined profile HMMs (capturing the properties of the repeating motif) and PHMMs (modeling alignments) into a single scoring scheme that can be decoded by a newly proposed algorithm. However, their scoring scheme is no longer a probabilistic model and the method is focused on correctly aligning individual occurrences of a single motif rather than alignment of long sequences interspersed with multiple motifs.

Here, we propose a simple tractable PHMM for sequence alignment with tandem repeats, and we explore various decoding methods for use of this model in sequence alignment. In addition to the classical Viterbi decoding, we define several variants based on the posterior decoding and block-based methods tailored to the specifics of our model. To demonstrate the differences, we have implemented several of these methods and compared their performance.

2 Pair HMM for Alignment with Tandem Repeats

Tandem repeats may arise by a complicated sequence of evolutionary events, including multiple rounds of tandem duplication, deletion, point mutation, gene conversion and other phenomena. Tandem repeat arrays at homologous locations in two related species may have arisen in the common ancestor and thus share part of their evolutionary history, but they could be further modified by independent events occurring after speciation. Models attempting to capture such diverse evolutionary mechanisms usually lead to complex problems in inference and parameter estimation. We propose a tractable model, based on classical PHMMs, which still captures the essence of a tandem repeat array: periodically repeating motif, which may be shared between the two species, or be specific for one species only.

A PHMM defines a probability distribution over alignments of two sequences X and Y . The standard PHMM has three states: match state M generating ungapped columns of the alignment, and two insert states I_X and I_Y , where I_X generates alignment columns with a symbol from X aligned to a gap, and I_Y generates columns with a symbol from Y aligned with a gap (Durbin et al., 1998). In our work, we will use a more complex PHMM, but standard algorithms for inference in these models are still applicable.

We call our model SFF and its details are shown in Fig.1. The model contains a standard three-state PHMM and two “sunflower” submodels $R_{i,X}$ and $R_{i,Y}$ for each possible repeating motif i . Submodel $R_{i,X}$ generates several (possibly zero) copies of the motif in sequence X and submodel $R_{i,Y}$ generates motif copies in sequence Y . Each copy of the motif is generated independently and the number of copies in X and Y are independent and geometrically distributed.

Each sunflower submodel is a circularized profile HMM emitting copies of the motif in one of the two sequences. For a motif of length p , the submodel contains p match states M_0, \dots, M_{p-1} , each match state emitting one symbol of the motif. Insertion state I_j allows to insert additional characters between symbols emitted by M_j and $M_{(j+1) \bmod p}$. Deletion states D_j and D'_j allow to bypass match state M_j , and thus correspond to deletions with respect to the reference motif sequence. Since the submodel can emit multiple tandem copies of the motif, the states in column $p - 1$ are connected to the states in column 0. To avoid cycles consisting solely of silent states, we use two separate chains of deletion states. Chain D'_0, \dots, D'_{p-2} can be entered only in state D'_0 , and model can stay in this chain for at most $p - 1$ steps. Chain D_1, \dots, D_{p-1} can be entered only after visiting at least one match or insert state in the current

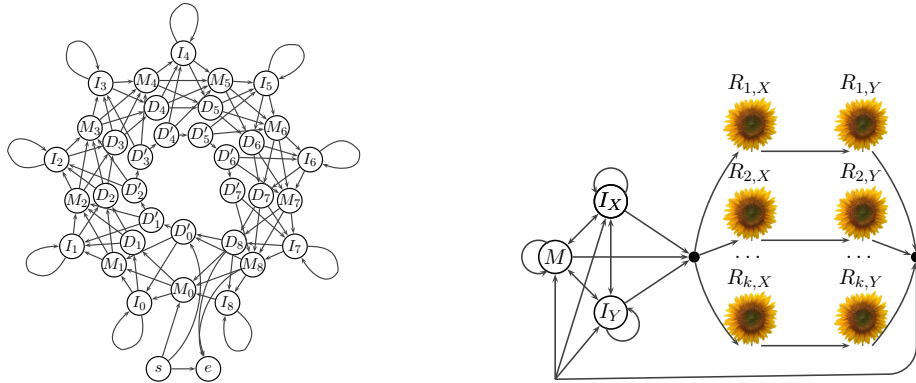


Fig. 1. SFF (sunflower field) model: a pair hidden Markov model for alignment with tandem repeats. Each submodel $R_{i,\alpha}$ (left) is a circular profile hidden Markov model emitting tandem copies of the motif in one sequence. State M_j is the match state generating j th symbol of the motif, state I_j allows insertions between symbols j and $j+1$ of the motif, and states D_j and D'_j allow to skip state M_j . States s and e designate the entry and exit points from the submodel. The full SFF model (right) contains a standard three-state PHMM with states M, I_X and I_Y , and two submodels $R_{i,X}, R_{i,Y}$ for each motif i . States and submodels with subscript X and Y generate symbols in the respective sequence X or Y only.

copy of the motif. As a result, the model can never pass around the whole circle using delete states. Note that the model prefers integer number of repeats, even though partial repeat occurrences are common in the real data. If desired, this can be addressed by simple changes in the model topology or parameters.

The overall model can have sunflower submodels for an arbitrary number of motifs; we can even define an infinite model, in which every possible finite string serves as the consensus for one pair of sunflowers. In our work, we use $k = 310,091$ motifs chosen as consensus strings of all tandem repeats found by the TRF program (Benson, 1999) run on the human chromosome 15 and its homologous sequences in the dog genome. The probability of choosing a particular motif out of all k possibilities can be uniform or dependent on the motif length or composition. We assign this probability based on the observed frequency of the corresponding consensus pattern in the TRF output. Alternatively, we could use a much smaller model by Frith (2011); however, this model does not easily handle insertions and deletions within repeats.

Likewise, we could use a multiple alignment of real motif occurrences to set individual parameters of the profile HMM. Instead, we use the same set of parameters for all states of all motif submodels. In particular, we set the insert and delete rates to 0.005; the match states allow mutations away from consensus according to the Jukes-Cantor model with parameter $t = 0.05$. Parameters of

X:	A	C	-	-	-	-	T	a_i :	1	2	-2	-2	-2	-2	3
Y:	-	C	G	A	A	A	T	b_i :	-0	1	2	3	4	5	6
								s_i :	I_X	M	I_Y	r	r	r	R
								r_i :	0	0	0	1	1	1	0

Fig. 2. Example of an alignment represented in our notation, together with its state and repeat annotation. Assuming that submodel $R_{1,Y}$ in the SFF model represents consensus sequence A, state r in the state sequence is a shorthand for the state M_1 within $R_{1,Y}$.

the three-state PHMM were estimated from the UCSC alignment of the human chromosome 15 and its homologous regions in the dog genome.

Our model also assumes that individual copies of a fixed motif are independent. If they share part of their evolutionary history, this assumption is not valid, but it greatly simplifies the model. We could add some limited dependence by introducing repeat submodels emitting copies in the two sequences simultaneously; we have used such a model in a different setting in our previous work (Kováč et al., 2012).

3 Inference Criteria and Algorithms

Given the SFF model introduced in the previous section, and two sequences $X = x_1 \dots x_n$ and $Y = y_1 \dots y_m$, we wish to find the alignment of these two sequences best agreeing with the model. We can also annotate this alignment by labeling individual alignment columns with additional information. We start by defining an alignment and its annotation more formally (see Fig.2). An *alignment* of X and Y is a sequence of pairs $(a_1, b_1), \dots, (a_t, b_t)$, each pair representing one alignment column. Symbol a_i represents either a position in X , or a gap annotated with the position of the nearest non-gap symbol on the left; formally $a_i \in \{1, \dots, n\} \cup \{-0, -1, \dots, -n\}$. To specify a valid alignment, a_1 must be 1 or -0 , a_t must be n or $-n$, and if $a_i \in \{j, -j\}$, a_{i+1} must be $j+1$ or $-j$. The conditions on symbols b_i representing positions in sequence Y are analogous. The *state annotation* of an alignment is a sequence of states $s_1 \dots s_t$ such that state s_i generated alignment column (a_i, b_i) . The *repeat annotation* is a binary sequence $r_1 \dots r_t$, where $r_i = 1$ if the state s_i generating the i -th column is one of the states in the repeat submodels. While the state annotation can be used with any PHMM generating the alignment, the repeat annotation is appropriate only for the SFF model or other PHMMs explicitly modeling repeats.

We will explore several inference criteria for choosing the best alignment. To describe them, we will use the terminology of gain functions (Hamada et al., 2009); analogous notion of a loss functions is frequently used for example in statistics and machine learning. A *gain function* $G(A, A_T)$ evaluates similarity between a predicted alignment A and the correct alignment A_T ; higher gain meaning that the prediction is of higher quality. Since the true alignment A_T is not known, we will consider the expected gain $E_{A_T}[G(A, A_T)|X, Y]$ of alignment

A , assuming that sequences X and Y were generated by our model

$$E_{A_T}[G(A|A_T)|X, Y] = \sum_{A_T} G(A, A_T) \Pr(A_T|X, Y).$$

In each optimization criterion, we choose a particular gain function and look for alignment A^* maximizing the expected gain $A^* = \arg \max_A E_{A_T}[G(A, A_T)|X, Y]$. Note that the gain function is only a way of defining the optimal solution; the corresponding decoding algorithm needs to be designed on a case-by-case basis.

3.1 Decoding Criteria for the Three-State PHMM

For simplicity, we start with criteria for the three-state PHMM, where the state annotation is uniquely determined by the alignment itself.

Viterbi decoding. Perhaps the simplest gain function assigns gain +1 if the predicted alignment A is identical to the true alignment A_T , and 0 otherwise. To optimize this gain function, we need to find the alignment with the highest overall probability in the model. In the simple three-state PHMM, this alignment can be found by the classical Viterbi algorithm in time $O(nmE)$, where E is the number of non-zero transitions in the model.

Posterior decoding. While the Viterbi decoding assigns gain only if the whole alignment is correctly predicted, posterior decoding assigns gain +1 for each correctly identified alignment column. Recall that the column is a pair (a_i, b_i) , and it is considered correct, if the same column also occurs somewhere in the true alignment. The optimal alignment under this gain function can be found by computing the posterior probability of each alignment column using the forward and backward algorithms for PHMMs, and then finding the alignment as a collection of compatible columns with the highest sum of posterior probabilities. A similar algorithm is considered for example by Lunter et al. (2008), except that the column posteriors are multiplied rather than added. The running time of this algorithm is again $O(nmE)$.

Marginalized posterior decoding. Lunter et al. (2008) also consider a variant of posterior decoding, where a column $(i, -j)$ is considered correct and receives a gain +1, if the true alignment contains a column $(i, -\ell)$ for any value of ℓ . In other words, when symbol x_i is aligned to a gap, we do not distinguish where is the location of this gap with respect to sequence Y . Columns $(-j, i)$ are treated symmetrically. To optimize this gain function, we again start by computing posteriors of all columns. Then we marginalize the probabilities of gap columns, effectively replacing posterior of column $(i, -j)$ with the sum of posteriors of columns $(i, -\ell)$ for all ℓ . As before, we then find the alignment maximizing the sum of posteriors of its columns. The algorithm runs in $O(nmE)$ time.

3.2 Decoding Criteria for the SFF Model

In more complex models, including ours, one alignment can be generated by several different state paths. Various gain functions can thus take into account also the state or repeat annotation of the alignment.

Viterbi decoding. In more complex models, the classical Viterbi algorithm optimizes a gain function in which the alignment is annotated with the state path generating it, and gain is awarded only when both the alignment and the state path are completely correct.

Posterior and marginalized posterior decoding. We will consider a variant of the posterior decoding, in which alignment columns are annotated by the repeat annotation, and an alignment column gets a gain +1, if the true alignment contains the same column with the same label. The only change in the algorithm is that the forward-backward algorithm produces posterior probabilities of columns annotated with the state, which are then marginalized over all states with the same repeat label. The running time is still $O(nmE)$. Similar modification can be done for marginalized posterior decoding, where we marginalize gap columns based on both state and gap position.

Block decoding. We will consider also a stricter gain function, which requires that repeat regions have correctly identified boundaries. We will split the alignment annotated with repeats into *blocks*, so that each maximal region of consecutive columns labeled as a repeat forms a block. Each column annotated as a non-repeat also forms a separate block. The gain function awards gain +1 for each non-gap symbol in every correctly predicted and labeled block. Correctness of non-repeat columns is defined as in posterior decoding. A repeat block is considered correct, if exactly the same region in X and the same region in Y are also forming a repeat block in the true alignment. Note that the gain for each block is proportional to the number of non-gap symbols in the block to avoid biasing the algorithm towards predicting many short blocks.

To optimize this gain function, we first compute posterior probabilities for all blocks. Note that a block is given by a pair of intervals, one in X and one in Y . Therefore the number of blocks is $O(n^2m^2)$. The expected gain of a block is its posterior probability multiplied by the number of its non-gap symbols. After computing expected gains of individual blocks, we can find the highest scoring combination of blocks by dynamic programming in $O(n^2m^2)$ time.

To compute block posterior probabilities, we transform the SFF model to a generalized PHMM (Pachter et al., 2002), in which all repeat states are replaced by a single generalized state R . In generalized HMMs, emission of a state in one step can be an arbitrary string, rather than a single character. In our case, the new state R generates a pair of sequences from the same distribution as defined by one pass through the repeat portion of the original SFF model. Pair of sequences generated by R represents one block of the resulting alignment. We call this new model the block model. Using the forward-backward algorithm

for generalized HMMs, we can compute posterior probabilities of all blocks in $O(n^2m^2f)$ time where f is the time necessary to compute emission probability for one particular block.

If we naively compute each emission separately, we get $f = O(nmE)$. However, we can reduce this time as follows. If the SFF contains only one motif, the emission probability of sequences x and y in the R model is simply

$$\Pr(x, y | R) = \Pr(x | R_{1,X}) \Pr(y | R_{1,Y}),$$

because the model first generates x in the sunflower submodel $R_{1,X}$ and then generates y in the model $R_{1,Y}$. Note that these two models are connected by a transition with probability 1. In the general case, we sum the probabilities for all k motifs, each multiplied by the transition probability of entering that motif. To compute block emission probabilities fast, we precompute $\Pr(x | R_{i,X})$ and $\Pr(y | R_{i,Y})$ for all substrings x and y of sequences X and Y respectively. This can be done by the forward algorithm in $O((n^2 + m^2)E)$ time. After this preprocessing, the computation of emission probability is $O(k)$, and the overall running time of this algorithm is $O(kn^2m^2 + (n^2 + m^2)E)$.

Block Viterbi decoding. The final gain function we consider is a variant of the Viterbi decoding. The Viterbi decoding assigns gain +1 for a completely correct alignment labeled with a correct state annotation. One alternative is to assign gain +1 if the alignment and its repeat annotation are completely correct. This gain function considers as equivalent all state paths that have the same position of repeat boundaries but use different motifs or different alignments of the sequence to the motif profile HMM.

In the SFF model, location of a repeat block uniquely specifies alignment within the block, because all symbols from sequence X must come first (aligned to gaps), followed by symbols from sequence Y . However, some models may emit repeat bases from the two sequences aligned to each other. We wish to abstract from exact details of repeat alignment, and consider different alignments within a repeat as equivalent. Therefore, we will reformulate the gain function in terms of blocks. The alignment labeled with repeat annotation gets a gain 1, if all its blocks are correct, where block correctness is determined as in the block decoding. This formulation is similar to the one solved by Hudek (2010).

To optimize this gain function, we use the Viterbi algorithm for generalized HMMs applied to the block model, which leads to running time $O(kn^2m^2 + (n^2 + m^2)E)$, by similar reasoning as above.

3.3 Practical considerations

Even the fastest algorithms described above require $O(nmE)$ time, where sequence lengths n and m can be quite high when aligning whole syntenic genomic regions and the size of the model E depends on the sum of the lengths of all repeat motifs, which can be potentially even infinite. However, we can use several heuristic approaches to make the running times reasonable.

First of all, we can use the standard technique of banding, where we restrict the alignment to some window around a guide alignment obtained by a faster algorithm. A simpler form of banding is to split the guide alignment to non-overlapping windows and realign each window separately. These techniques reduce the $O(nm)$ factor.

To restrict the size of the model, we first find tandem repeats in X and Y independently by running the TRF program (Benson, 1999). Then we include in our model only those motifs which appear at least once in the TRF output. If we process only relatively short windows of the banded alignment, the size of the model will be quite small. Note however, that we keep the transition probabilities entering these models the same as they are in the full SFF model. If TRF finds a consensus not included in the original SFF model, we add its two submodels with a small probability comparable to the rarest included motifs.

These two heuristics sufficiently speed up algorithms running in $O(nmE)$ time. The block decoding and the block Viterbi decoding need to consider all possible blocks, which is prohibitive even within short alignment windows. Therefore, we limit possible repeat blocks only to intervals discovered as repeats by the TRF program. We allow the generalized repeat state R to generate the block of substrings x and y if each of these substrings is either empty or one of the intervals found by TRF has both its endpoints within 10 bases from the respective endpoints of x or y . Therefore, if TRF finds t_X intervals in X and t_Y intervals in Y , we try at most $(20t_X + n)(20t_Y + m)$ blocks.

The final consideration is that the SFF model does not align tandem repeats at orthologous locations, even if they share a common evolutionary history. This might be impractical for further use. Therefore we postprocess the alignments by realigning all blocks annotated as repeats using the standard three-state PHMM. In this realignment, we also include gaps adjacent to these repeats.

4 Experiments

We have compared decoding methods described in the previous section and several baseline algorithms on simulated data (see Table 1). The data set contained 200 alignments of length at least 200 each generated from the SFF model (the same model parameters were used in the sampling and for the alignments). In generating the dataset, we required that each tandem repeat had at least three copies in both species; otherwise, we would obtain many regions that would be labeled as tandem repeats, but would in fact only have a single copy. The error rate (the first column of the table) measures the fraction of true alignment columns that were not found by a particular algorithm. It was measured only on the alignment columns that were generated from non-repeat states in the simulation, as the SFF model does not give any alignment in repeat regions.

The first observation is that the methods based on the SFF model (the first block of the table) outperform the baseline method (the Viterbi algorithm on the three-state model), reducing the error rate by 10–30%. In general, the methods that score individual alignment columns are more accurate than the block-based

Table 1. Accuracy of several decoding methods on simulated data. *: method uses the real consensus motifs. **: method uses the real consensus motifs and intervals from the real repeat blocks.

Algorithm	Alignment	Repeat		Block	
	error	sn.	sp.	sn.	sp.
SFF marginalized	3.37%	95.97%	97.78%	43.07%	44.87%
SFF posterior	3.53%	95.86%	97.87%	42.70%	47.37%
SFF block	3.87%	91.20%	98.04%	36.13%	47.14%
SFF block Viterbi	4.32%	91.28%	97.96%	35.40%	45.97%
SFF Viterbi	4.04%	95.29%	97.85%	42.70%	48.95%
SFF marginalized*	3.02%	98.93%	99.64%	77.01%	76.17%
SFF posterior*	3.42%	98.84%	99.51%	75.91%	80.93%
SFF block**	3.21%	97.70%	99.87%	80.66%	94.44%
SFF block Viterbi**	3.71%	98.12%	99.85%	81.75%	92.18%
SFF Viterbi*	3.94%	98.54%	99.45%	75.55%	83.47%
Context	5.98%				
Muscle	5.62%				
3-state posterior	4.41%				
3-state Viterbi	4.78%				

or the Viterbi-based methods, which is not surprising, because error rate as a measure of accuracy is closer to the gain function they optimize. We have also compared our approach to the related method of context-sensitive indels (Hickey and Blanchette, 2011). The Context program was trained on a separate set of 200 alignments sampled from our model. However, its error rate is quite high, perhaps due to insufficient training data or some software issues. Finally, we have also run the Muscle aligner with default parameters (Edgar, 2004); we have used the result as a guide alignment for the slower block-based decoding methods (the new alignment was restricted to be within 30 base window from the guide alignment).

The SFF-based algorithms use the tandem repeat motifs predicted by the TRF, as well as approximate repeat intervals (block-based methods). The TRF predictions are not exact and may contribute to the overall error rate. We attempted to quantify this effect by using the real tandem repeat motifs and real boundary positions instead of the TRF predictions (the second block of Table 1). We can see that the use of TRF predictions indeed leaves space for improvement, with the best performing algorithm reducing the error rate by almost 40% compared to the baseline. Block-based methods work significantly better with true intervals than with the TRF intervals, suggesting that further improvements in repeat interval detection are needed.

The decoding methods that use the SFF model produce an alignment and a repeat annotation. Comparing annotation of each base in both sequences with the true repeat annotation sampled from the model (table columns repeat sensitivity and specificity), we note that the marginalized posterior decoding is the most sensitive, and the block decoding the most specific method. Specificity was

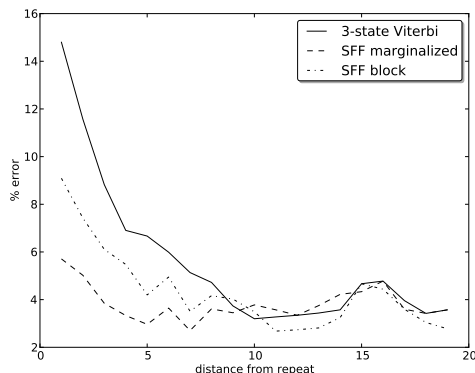


Fig. 3. Alignment error rate of three decoding methods as a function of the distance from the nearest repeat.

quite high for all methods, low sensitivity for block-based methods was probably caused by wrong repeat intervals predicted by the TRF, since it improves markedly by using correct intervals.

We also compared the accuracy of predicting repeat block boundaries (table columns block sensitivity and specificity). The number of blocks with correctly predicted boundaries is quite low, most likely because there are usually many high-probability alternatives with slightly shifted boundaries. However, even though more than half of the repeat blocks have some error in the boundary placement, the SFF-based methods improve the alignment accuracy most markedly close to repeat boundaries, as shown in Fig.3. This is expected, because far from repeats the model works similarly to the three-state PHMM.

To illustrate the feasibility of running our methods on real genomic data, we have realigned the 1.8Mb CFTR region on the human chromosome 7 to orthologous portions of the dog genome. We have started with the lastz alignment (Harris, 2007) downloaded from the Ensemble website (Flicek et al., 2013). We have then run the TRF program on both species and selected alignment windows of length 50–350 that contained at least one repeat. Regions without repeats or with very long repeats were left with the original alignment. Using the block decoding with the SFF model, we have thus realigned windows covering roughly 70% of the original alignment. About 8% of all alignment columns were annotated as repeats.

5 Conclusion

We have designed a new pair hidden Markov model for aligning sequences with tandem repeats and explored a variety of decoding optimization criteria for its use. The new model coupled with appropriate decoding algorithm reduces the

error rate on simulated data, especially around boundaries of tandem repeats. With suitable heuristics, our approach can be used to realign long genomic regions.

Our experiments are the first study comparing a variety of different decoding criteria for PHMMs. Our criteria for the SFF model optimize both the alignment and the repeat annotation. Depending on the application, one or the other may be of greater interest, and thus one may want to marginalize over all alignments and optimize the annotation, as in (Satija et al., 2010), or marginalize over labels and optimize the alignment.

Our model does not take into the account the dependencies between the repeat occurrences in the two species. A tractable model allowing such dependencies would be of great interest. Previously, we have explored the problem of aligning two sequences simultaneously to a profile HMM, but we were not able to design a simple generative model for this purpose (Kováč et al., 2012).

Acknowledgements. This research was funded by VEGA grant 1/1085/12.

Bibliography

- Benson, G. (1997). Sequence alignment with tandem duplication. *Journal of Computational Biology*, 4(3):351–357.
- Benson, G. (1999). Tandem repeats finder: a program to analyze DNA sequences. *Nucleic Acids Research*, 27(2):573–580.
- Bérard, S., Nicolas, F., Buard, J., Gascuel, O., and Rivals, E. (2006). A fast and specific alignment method for minisatellite maps. *Evolutionary Bioinformatics Online*, 2:303.
- Durbin, R., Eddy, S., Krogh, A., and Mitchison, G. (1998). *Biological sequence analysis: Probabilistic models of proteins and nucleic acids*. Cambridge University Press.
- Edgar, R. C. (2004). MUSCLE: multiple sequence alignment with high accuracy and high throughput. *Nucleic Acids Research*, 32(5):1792–1797.
- Flicek, P. et al. (2013). Ensembl 2013. *Nucleic Acids Research*, 41(D1):D48–D55.
- Freschi, V. and Bogliolo, A. (2012). A lossy compression technique enabling duplication-aware sequence alignment. *Evolutionary Bioinformatics Online*, 8:171.
- Frith, M. C. (2011). A new repeat-masking method enables specific detection of homologous sequences. *Nucleic Acids Res*, 39(4):e23.
- Gemayel, R., Vincens, M. D., Legendre, M., and Verstrepen, K. J. (2010). Variable tandem repeats accelerate evolution of coding and regulatory sequences. *Annual Review of Genetics*, 44:445–477.
- Hamada, M., Kiryu, H., Sato, K., Mituyama, T., and Asai, K. (2009). Prediction of RNA secondary structure using generalized centroid estimators. *Bioinformatics*, 25(4):465–473.
- Harris, R. (2007). *Improved pairwise alignment of genomic DNA*. PhD thesis, Pennsylvania State University.

- Hickey, G. and Blanchette, M. (2011). A probabilistic model for sequence alignment with context-sensitive indels. *Journal of Computational Biology*, 18(11):1449–1464.
- Holmes, I. and Durbin, R. (1998). Dynamic programming alignment accuracy. *Journal of Computational Biology*, 5(3):493–504.
- Hudek, A. K. (2010). *Improvements in the Accuracy of Pairwise Genomic Alignment*. PhD thesis, University of Waterloo, Canada.
- Kováč, P., Brejová, B., and Vinař, T. (2012). Aligning sequences with repetitive motifs. In *Information Technologies - Applications and Theory (ITAT)*, pages 41–48.
- Lunter, G., Rocco, A., Mimouni, N., Heger, A., Caldeira, A., and Hein, J. (2008). Uncertainty in homology inferences: assessing and improving genomic sequence alignment. *Genome Research*, 18(2):298–309.
- Messer, P. W. and Arndt, P. F. (2007). The majority of recent short DNA insertions in the human genome are tandem duplications. *Mol Biol Evol*, 24(5):1190–1197.
- Miyazawa, S. (1995). A reliable sequence alignment method based on probabilities of residue correspondences. *Protein Engineering*, 8(10):999–1009.
- Needleman, S. B. and Wunsch, C. D. (1970). A general method applicable to the search for similarities in the amino acid sequence of two proteins. *Journal of Molecular Biology*, 48(3):443–443.
- Pachter, L., Alexandersson, M., and Cawley, S. (2002). Applications of generalized pair hidden Markov models to alignment and gene finding problems. *Journal of Computational Biology*, 9(2):389–399.
- Sammeth, M. and Stoye, J. (2006). Comparing tandem repeats with duplications and excisions of variable degree. *IEEE/ACM Transactions on Computational Biology and Bioinformatics*, 3(4):395–407.
- Satija, R., Hein, J., and Lunter, G. A. (2010). Genome-wide functional element detection using pairwise statistical alignment outperforms multiple genome footprinting techniques. *Bioinformatics*, 26(17):2116–2120.
- Schwartz, A. S. and Pachter, L. (2007). Multiple alignment by sequence annealing. *Bioinformatics*, 23(2):e24–e29.